Master's Thesis

Dynamic Transition of Mitochondrial Transcription from Initiation to Elongation Phase at Single Molecular Level

Byeong-Kwon Sohn

Department of Biomedical Engineering

Graduate School of UNIST

2019

Dynamic Transition of Mitochondrial Transcription from Initiation to Elongation Phase at Single Molecular Level

Byeong-Kwon Sohn

Department of Biomedical Engineering

Graduate School of UNIST

Dynamic Transition of Mitochondrial Transcription from Initiation to Elongation Phase at Single Molecular Level

A thesis/dissertation
submitted to the Graduate School of UNIST
in partial fulfillment of the
requirements for the degree of
Master of Science

Byeong-Kwon Sohn

12/3/2018

Approved by

Advisor
Hajin Kim

Dynamic Transition of Mitochondrial Transcription from Initiation to Elongation Phase at Single Molecular Level

Byeong-Kwon Sohn

This certifies that the thesis/dissertation of Byeong-Kwon Sohn is approved.

12/3/2018

signature

Advisor: Hajin Kim

signature

Jayil Lee: Thesis Committee Member #1

signature

Taejoon Kwon: Thesis Committee Member #2

Abstract

The gene expression in mitochondria starts with the assembly of the mitochondrial RNA polymerase and transcription factors to recognize promoter sequence. The dynamic control of these molecular machineries is crucial for the regulation of their active roles in cellular energy metabolism. Transcription is known to occur through distinct stages of initiation, elongation, and termination but it remains poorly understood how the transcription complex regulates the transition between the phases. Here, we report the first direct observation of the dynamics of mitochondrial transcription complex through initiation to elongation phases by single molecule fluorescence resonance energy transfer (smFRET) techniques, using the model organism of yeast *Saccharomyces cerevisiae.* The yeast mitochondrial RNA polymerase (Rpo41) and the transcription factor (Mtf1) initially open the promoter region and then progressively bend the DNA to sharper angle as they walk up to +7 position, during which they also scrunch the downstream DNA into the complex. At each stage, the initiation complex does not stay still but exhibits active bending-unbending and scrunching-unscrunching motions. At +8 position, an abrupt drop of the FRET level and disappearance of the dynamics occurs, marking the transition to the elongation phase where the DNA is in a stable, straight, and unscrunched form. Hidden Markov analysis of the smFRET traces revealed the dynamic features at each stage. We analyzed the roles of Mtf1 using truncated mutants, revealing that the C-terminal tail is responsible for stabilizing the scrunched initiation complex, hence regulating the branching between the transition to elongation phase and the abortive initiation.

Contents

I. Introduction ---------- 1

1.1 Mitochondrial transcription ---------- 1

1.2 Conformational dynamics of transcription complex ---------- 2

1.3 Phase transition from initiation to elongation ---------- 3

II. Materials & Method ---------- 4

2.1 Substrate DNA design ---------- 4

2.2 Preparation of proteins ---------- 5

2.3 smFRET measurements using TIRFM---------- 6

- Detailed procedure of PEGylation ---------- 7

III. Results ---------- 8

3.1 Conformational dynamics in transcription complex along the initiation --------- 8

3.2 Phase transition from initiation to elongation ---------- 9

3.3 Distinct level of FRET efficiency in position +8 complex ---------- 11

3.4 Hidden Markov Modelling analysis ---------- 12

3.5 Role of C-terminal tail of Mtf1 at initiation phase ---------- 14

3.6 NTP washing experiments ---------- 15

IV. Discussion & Conclusion ---------- 16

V. References ---------- 17

List of Figures

Figure 1. a) Ribbon diagram of T7 RNAP and POLRMT. b) Mechanism of the initial steps of transcription initiation by the human mitochondrial machinery.

Figure 2. Conformational change of initiation complex by the yeast mitochondrial machinery.

Figure 3. Conformational changes in the promoter DNA by T7 RNA polymerase during the initiation and the transition from initiation to elongation.

Figure 4. Schematic image of substrate design with the positions where the transcription can be stalled, and the NTP combinations required for the stop, and detail sequence information.

Figure 5. Chemical principle of PEGylation on the quartz slides and schematic of preparing sample channel for smFRET measurements.

Figure 6. Results from transcriptional walking experiments using wild-type Mtf1. (A) schematic drawing of transcription complex consists of Rpo41(purple), Mtf1(wine), and substrate DNA. (B) FRET histograms at each stalled position (0 to +8 and run-off). (C) Example traces showing different types of dynamics at position 0, +2, and +7.

Figure 7. Phase transition from initiation to elongation. (A) Histograms from position +7 and +8 that are showing abrupt drop of the FRET level and disappearance of the dynamics at position +8. (B) Colocalization of Cy3 labeled Mtf1 and Cy5 labeled DNA. Left panel is Cy3 channel, and right panel is Cy5 channel. Green and red dots are signals from Cy3 and Cy5, and yellow dots are colocalized spots. (C) Bar graphs showing change of the colocalization ratio after adding NTPs, at different stalled positions. The positions with asterisks show significant drop.

Figure 8. (A) Example traces from NTP flow-in experiments. The NTPs are added after 20 seconds from the beginning of the measurements (dashed line). First trace is coming from the position +7, second one is from position +8, and third one is coming from run-off condition.

Figure 10. Hidden Markov Modelling(HMM) analysis. (A) Example panel showing HMM analysis. Three states are assigned properly. Closed DNA state (cyan), opened DNA state (orange), and scrunched DNA state (purple). (B) Transition density plots (TDP) at each position. It shows the density of transition from one state to another.

Figure 11. (Table) The table shows the transition rates at each position from HMM analysis and plotted into bar graph. There are three states (state 1 closed DNA, state 2 opened DNA, and state 3 scrunched DNA) during transcription at each stalled position. (Bar graph) Comparison of transition rates among the three states at each position.

Figure 12. (A) FRET histograms from experiments using mutant D12-Mtf1 at each stalled position. (B) Example FRET trace from D12-Mtf1 measurements. (C) Transcription gel assay using γ^{32}-ATP as substrate of transcription. Three lines from left to right are 1 WT-, 2 D12-, and 3 D20-Mtf1 and this order repeats.

Figure 13. (A) FRET efficiency histograms from washing experiments. The histograms on the top row come from equilibrium states of 4 different stalled positions and run-off condition. The bottom part is showing population change in the histograms until 5 minutes after washing out the NTPs. (B) Graphs comparing change in the population of FRET efficiency population after the washing at each position.

Abbreviations

Rpo41	yeast mitochondrial RNA polymerase
Mtf1	mitochondrial transcription factor 1
T7 RNAP	T7 bacteriophage RNA polymerase
TIRFM	total internal reflection fluorescence microscopy
IC/EC	initiation complex/Elongation complex
SVA	succinimidyl valeric acid
smFRET	single molecule fluorescence resonance energy transfer
HMM	hidden Markov modelling
WT-Mtf1	wild-type Mtf1
D12-Mtf1	mutant Mtf1 with truncation of 12 amino acids from its C-terminus
D20-Mtf1	mutant Mtf1 with truncation of 20 amino acids from its C-terminus

I. Introduction

1.1 Mitochondrial transcription

Mitochondria are the eukaryotic organelles responsible for energy production through oxidative phosphorylation process. Mitochondrial proteins consist of genes mostly originating from host cells but several key proteins come from their own genome transcribed by their own transcription machinery. Thus, to regulate proper functioning of mitochondria, it is important to accurately control the gene expression of the mitochondria. Here, the mitochondrial transcription machinery in yeast, *Saccharomyces cerevisiae,* was observed by single molecule techniques. The machinery is known to be homologous to T7 bacteriophage, and human mitochondrial transcription. (Fig. 1a) They have different number of proteins involved in the machinery. T7 bacteriophage's is single-subunit where T7 RNAP works alone but for yeast and humans, they have two and three proteins respectively. Human have three proteins, POLRMT, TFAM, TFB2M. (Fig. 1b) Among them, POLRMT and TFB2M is very similar in their structure with the proteins in yeast, Rpo41 and Mtf1. Because of the homology, the model organism yeast can give us some ideas about the mechanisms in more complex systems.

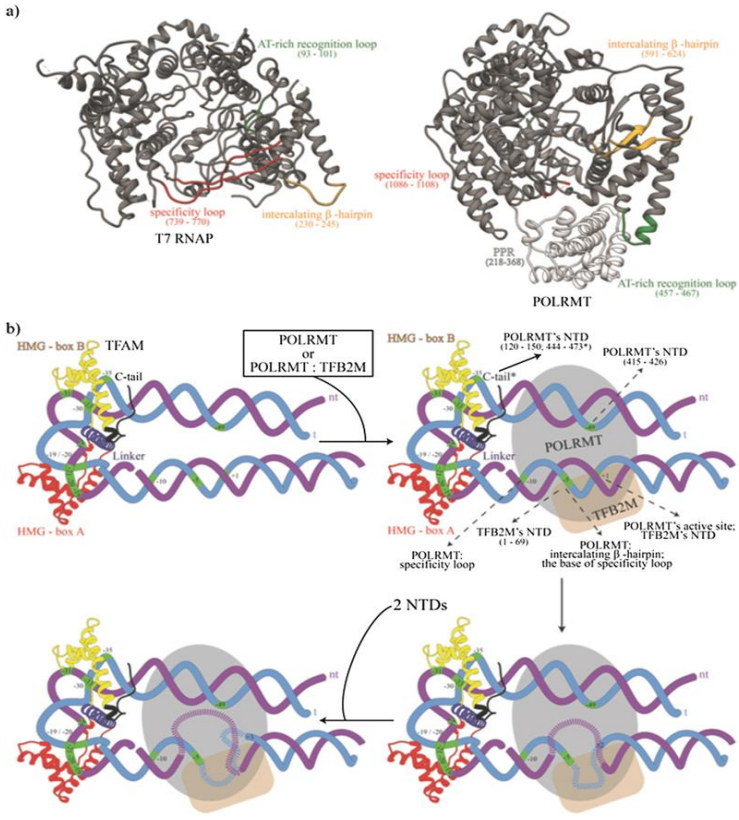

Drakulic, S., Cuellar, J., & Sousa, R. (2018). The Mitochondrial Transcription Machinery. In *RNA Metabolism in Mitochondria*(pp. 1-15). Springer, Cham.

Figure 1. a) Ribbon diagram of T7 RNAP and POLRMT. b) Mechanism of the initial steps of transcription initiation by the human mitochondrial machinery.

1.2 Conformational dynamics of transcription complex

Mitochondrial transcription involves only a handful of proteins but occurs through complicated and distinct stages of initiation, elongation, and termination, intervened by nonproductive, abortive initiation where incomplete short primers are produced during initiation instead of progressing to the elongation phase. By controlling the branching between abortive initiation and productive RNA synthesis, the expression level of proteins can be regulated but how the transcription machinery regulates the transition from initiation to elongation phase still remains poorly understood.

In this study, we employed single molecule techniques to measure the dynamics of the yeast mitochondrial transcription complex, in order to understand the transcription mechanism from molecular, mechanistic point of view.

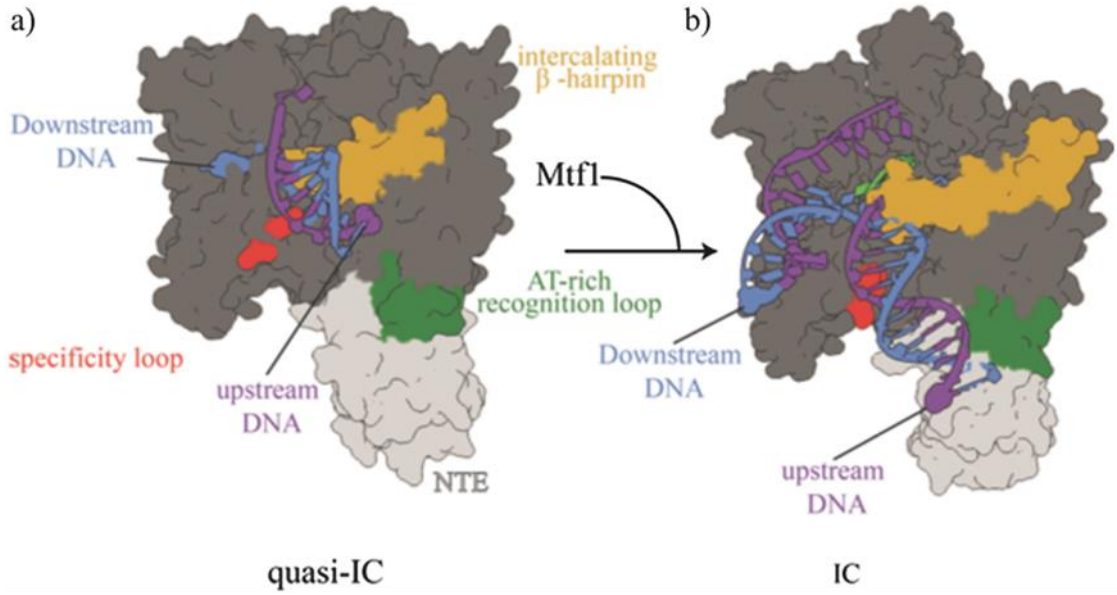

Drakulic, S., Cuellar, J., & Sousa, R. (2018). The Mitochondrial Transcription Machinery. In *RNA Metabolism in Mitochondria*(pp. 1-15). Springer, Cham.

Figure 2. Conformational change of initiation complex by the yeast mitochondrial machinery.

1.3 Phase transition from initiation to elongation

In the T7 RNA polymerase, a large structural change has been identified along with the phase transition from initiation to elongation in transcription (Fig 3). He concludes that conversion of IC to EC occurs after 8 bp to 12 bp synthesis of RNA in the T7 RNAP, by measuring FRET of upstream and downstream of promoter. Since then, we report for the first time, the direct observation of the dynamics of yeast mitochondrial transcription complex along the initiation phase and the transition to the elongation phase at the single molecular level. We show that the transcription complex progressively bends and scrunches the DNA during the initiation phase, during which it maintains and modulates the dynamics of bending-unbending and scrunching-unscrunching motions. At +8 position, a sharp transition to the elongation phase occurs, marked by the transformation of the DNA into more straight and stable form. The C-terminal domain of Mtf1 was found to regulate the branching between abortive initiation and elongation by controlling the stability of open promoter complex. Our findings provide novel mechanistic views of the mitochondrial transcription, which is crucial to understand the regulation mechanism of the mitochondrial gene expression and also to study more complicated transcription machineries of eukaryotic cells.

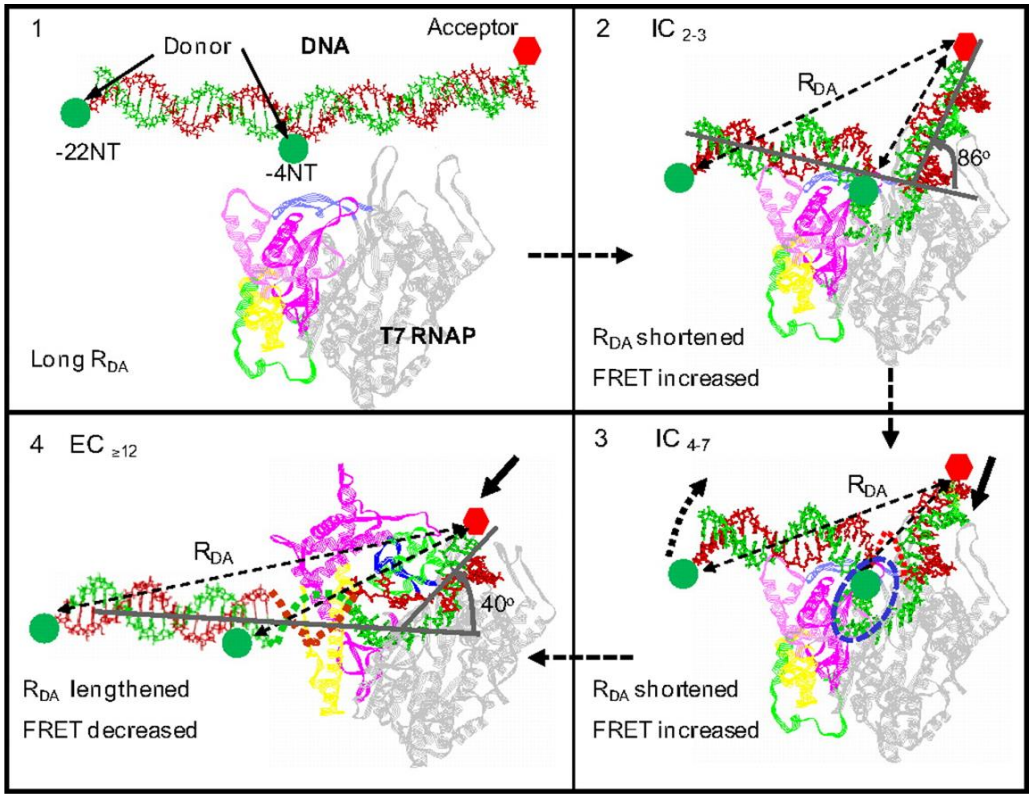

Guo-Qing Tang et al. PNAS 2009;106:52:22175-22180

Figure 3. Conformational changes in the promoter DNA by T7 RNA polymerase during the initiation and the transition from initiation to elongation.

II. Materials & Method

2.1 Substrate DNA design

We designed 50-basepair-long DNA substrates with promoter and handle sequence, fluorescently labeled at +16/-16 positions to measure the dynamic changes of the DNA conformation during transcription by smFRET techniques. Multiple DNA sequences were designed to pause the transcription complex at desired positions on the substrate using combinations of nucleotides and 3'-deoxynucleotides. All the DNAs were purchased and purified from Integrated DNA Technologies. The 50 bp long biotinylated template DNA strands have internal amine modifier on -16 position to label fluorescent dye, and their 50 bp long complementary non-template strands have amino modifier on their 3' end which is +16 position. The Cy5 and Cy3 dyes were labeled respectively using amine – NHS ester chemical reaction. After labeling, template and non-template DNAs were incubated at 94C for 5 min in annealing buffer (10 mM Tris-HCl, pH 8.0, 50 mM NaCl) and cooled to room temperature slowly to make double-stranded DNA.

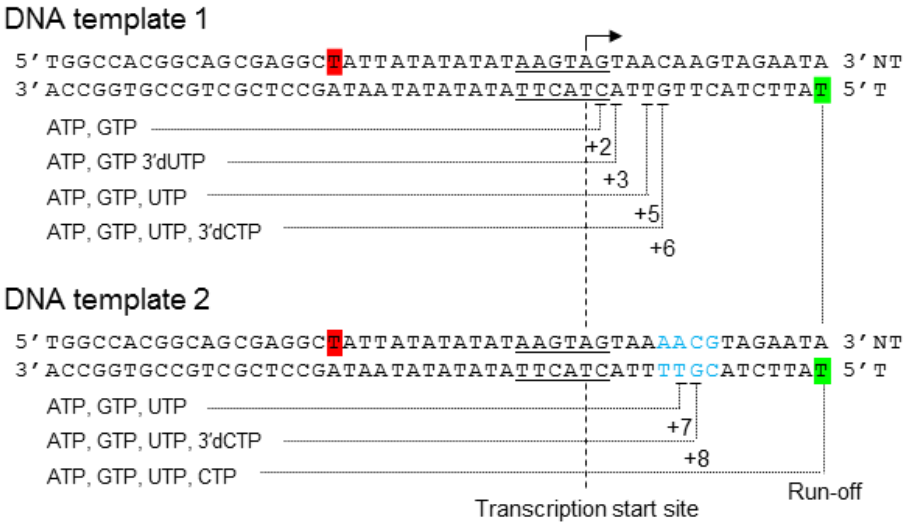

Figure 4. Schematic view of substrate design with the positions where the transcription can be stalled, and the NTP combinations required for the stop, and detail sequence information.

2.2 Preparation of proteins, Rpo41 and Mtf1

The expression and purification of yeast mitochondrial RNA polymerase, His-Rpo41 were carried out as previously described by Matsunaga *et al*. The expression and purification of the transcription factor in yeast mitochondria, N-HisMtf1, was carried out as described in previous report, Tang G.Q. *et al*. The proteins that were used in this research are expressed in *E.coli* and purified using successive Ni2+ Sepharose 6 Fast Flow, diethylaminoethyl-Sephacel (DEAE) and Heparin columns, from our collaborator Smita Patel Group, Department of Biochemistry and Molecular Biology, Rutgers – Robert Wood Johnson Medical School.

2.3 smFRET measurements using TIRFM

Quartz microscope slide glasses and coverslips are PEGylated before mounting the samples to minimize an effect of non-specific binding of DNA and proteins to the surface. First, the slides were functionalized with amine group by amino-silanization, then mPEG -SVA and biotin-PEG-SVA were

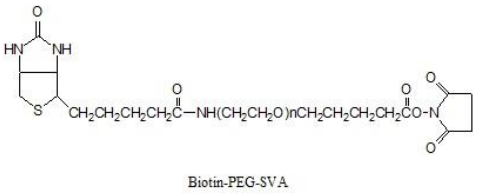

(Laysan bio, Inc.)

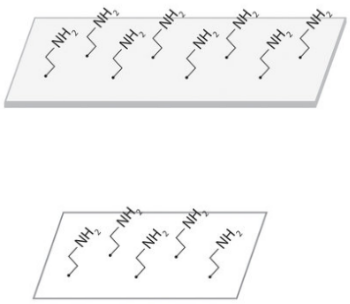

Chandradoss, S. D., Haagsma, A. C., Lee, Y. K., Hwang, J. H., Nam, J. M., & Joo, C. (2014). *Journal of visualized experiments: JoVE*, (86).

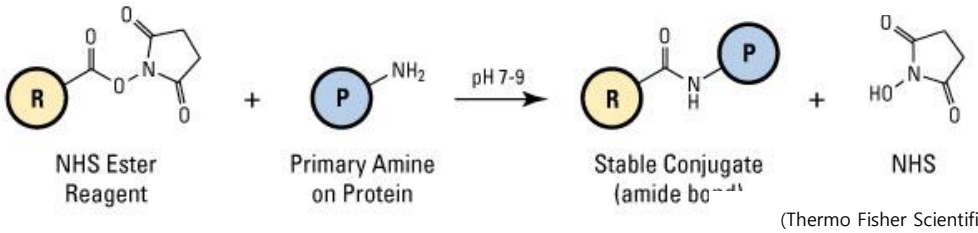

(Thermo Fisher Scientific)

introduced in molar ratio 40:1 by reaction between NHS-ester and amine group. Specific procedure for 'PEGylation' is below. After the PEGylation of quartz slide, chambers for sample injection were prepared using double-sided tape, epoxy, and cover glass (Fig 5).

Figure 5. Chemical principle of PEGylation on the quartz slides and schematic of preparing sample channel for smFRET measurements.

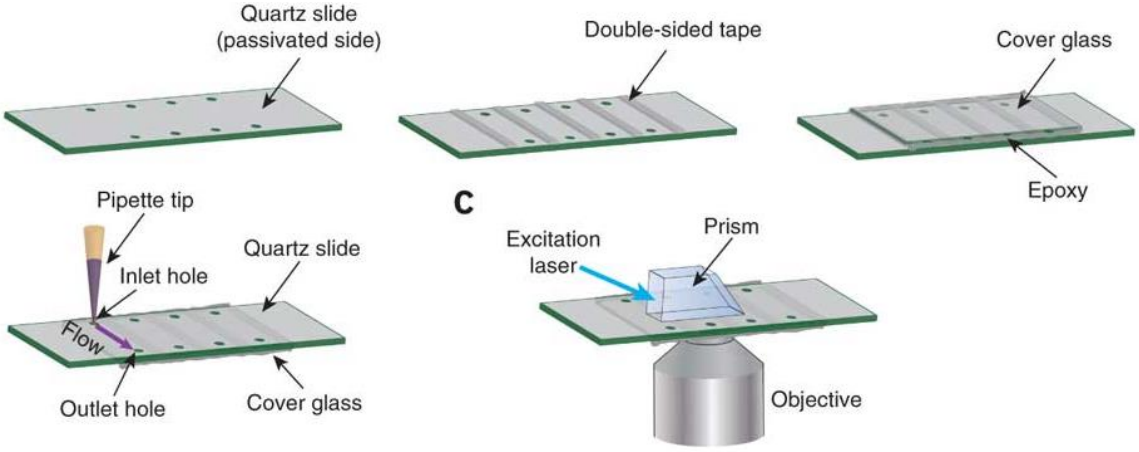

PEGylation procedure

1. Rinse quartz microscope slides and cover slips with acetone using sonicator for 1 hour. Rinse the slides several times repeatedly with dH2O.
2. Rinse the slides with 1M KOH more than 20 minutes using sonication. Rinse the slides several times repeatedly with dH2O.
3. Remove all the remaining organic molecules by burning the slides with torch.
4. Place the slides in methanol for 10 minutes.
5. Prepare a solution to functionalize the surface of the quartz slide with amine group.

   300mL Methanol, 15mL acetic acid, 3mL N-(2-Aminoethyl)-3-aminopropyltrimethoxysilane
6. Immerse the slides to the solution made in step 4, and incubate for 10 minutes, 1 min sonication, and incubate 10 minutes again.
7. Dissolve mPEG-SVA and biotin-PEG-SVA with 40:1 in molar ratio to filtered sodium bicarbonate buffer. Dissolve the PEG-SVA powders right before introducing to the slides (half-life of the SVA group in aqueous solution is about 30 minutes).
8. Apply the PEG solution on the one side of the cleaned, functionalized quartz slides and cover the solution by cover slips. Place the slides dark, even place and incubate 6 hours or overnight.
9. Detach the cover slips from the quartz slides and rinse them using dH2O. Make sure the surface is well-prepared during rinsing, because PEGylated surface is much hydrophobic than normal surface (it makes water droplet more round shape).
10. Dry the slides and coverslips and store them in dark -20C fridge after packing with vacuum packing system.

III. Results

3.1 Conformational dynamics in transcription complex along the initiation

The DNA substrates with promoter sequence, fluorescently labeled at +16/-16 positions to measure the dynamic changes of the DNA conformation during transcription by smFRET techniques (Fig 3-1). Multiple DNA sequences were designed to pause the transcription complex at desired positions on the substrate using combinations of nucleotides and 3'-deoxynucleotides. Interestingly, even at later stalled positions, FRET traces still exhibited dynamics transitions, representing the bending-unbending and scrunching-unscrunching dynamics (Fig 3B). FRET histograms measured at each stalled position revealed stepwise shift of the high FRET level, reflecting the progressive bending of the DNA, accompanied by scrunching, during the initiation phase (Fig. 3A, C).

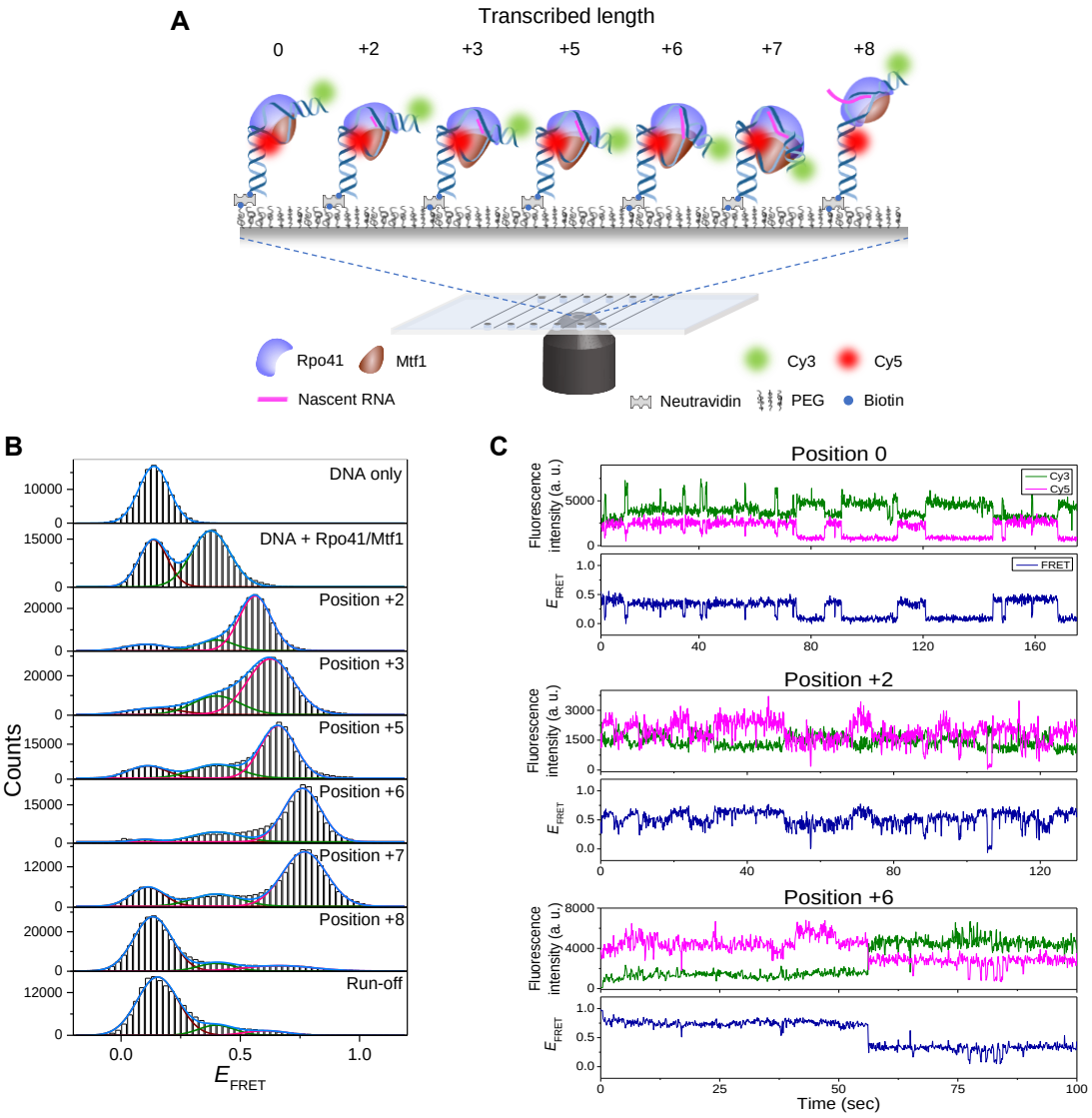

Figure 6. Results from transcriptional walking experiments using wild-type Mtf1. (A) schematic drawing of transcription complex consists of Rpo41(purple), Mtf1(wine), and substrate DNA. (B) FRET histograms at each stalled

position (0 to +8 and run-off). (C) Example traces showing different types of dynamics at position 0, +2, and +7.

3.2 Phase transition from initiation to elongation

Remarkably, the high FRET population at +7 position completely disappeared as we progressed to +8 position (Fig. 7A). This result implies that an abrupt structural change occurred at this step. Based on a report on T7 bacteriophage transcription system, we can interpret this as the collapse of initiation bubble in transition to the elongation phase, which results in the unbending and unscrunching of the DNA and facilitates clearing from the promoter region. Additional experiments using Cy3-labeled Mtf1 and Cy5 labeled DNA substrate showed the dissociation of Mtf1 at this stage, further validated the interpretation (Fig 7B & C).

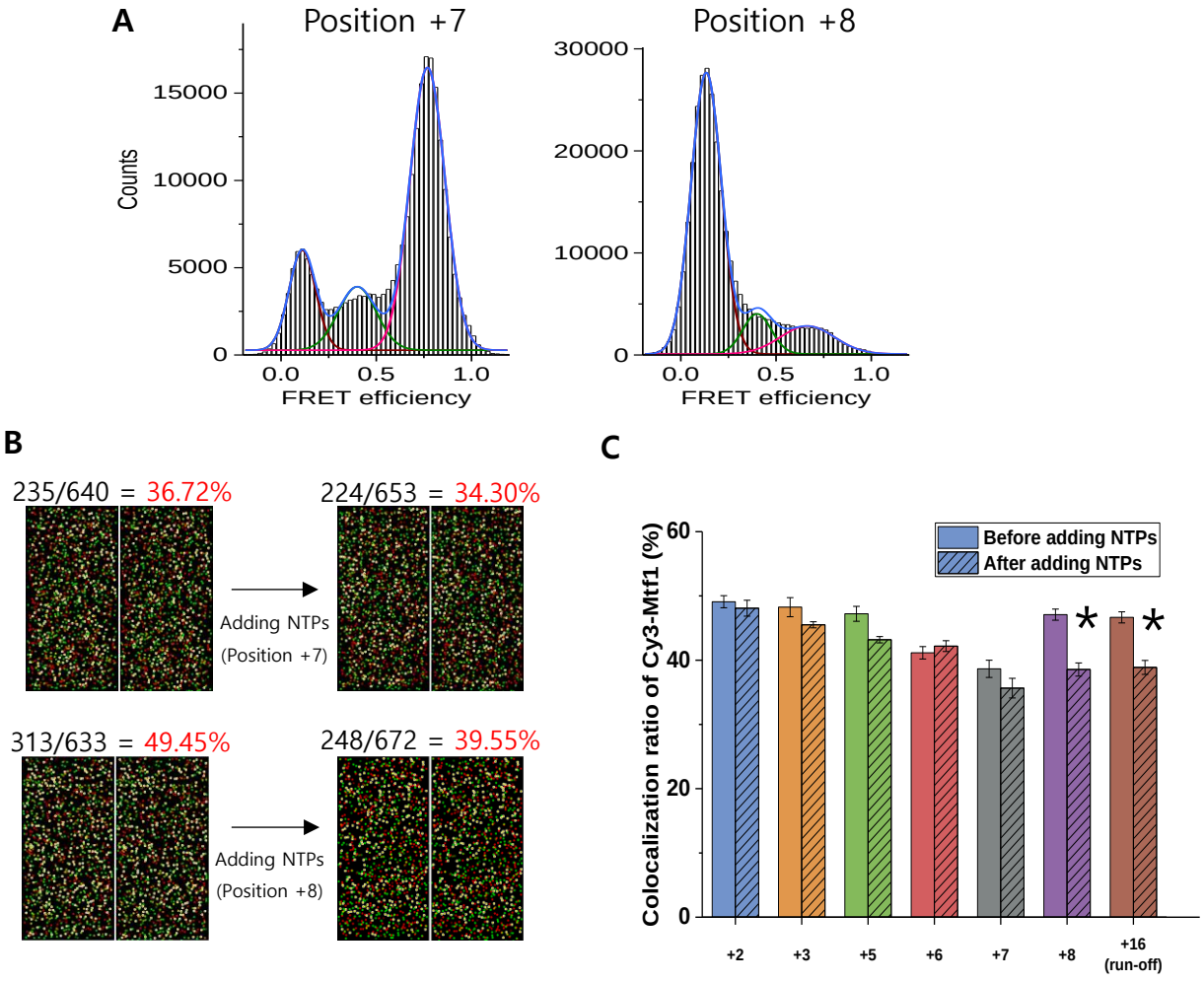

Figure 7. Phase transition from initiation to elongation. (A) Histograms from position +7 and +8 that are showing abrupt drop of the FRET level and disappearance of the dynamics at position +8. (B) Colocalization of Cy3 labeled Mtf1 and Cy5 labeled DNA. Left panel is Cy3 channel, and right panel is Cy5 channel. Green and red dots are signals from Cy3 and Cy5, and yellow dots are colocalized spots. (C) Bar graphs showing change of the colocalization ratio after adding NTPs, at different stalled positions. The positions with asterisks show significant drop.

From real time flow-in of NTP mix, we could trace the stepwise increase of FRET level followed by this drop (Fig. 8A). In the case of position +8, the FRET efficiency increased right after adding NTPs like position +7. Unlike the position +7, the efficiency abruptly decreases to 0.15 at time point 60 second. In the run-off condition, we observed multiple rounds of transcription which can be visualized by decrease of FRET efficiency after the increase which is shown right after the flow-in of NTPs and again in 70 second. The sudden drop of FRET efficiency after increases is also shown in population map (Fig. 8B). In the position +7, the high FRET level can be maintained longer time than position +8.

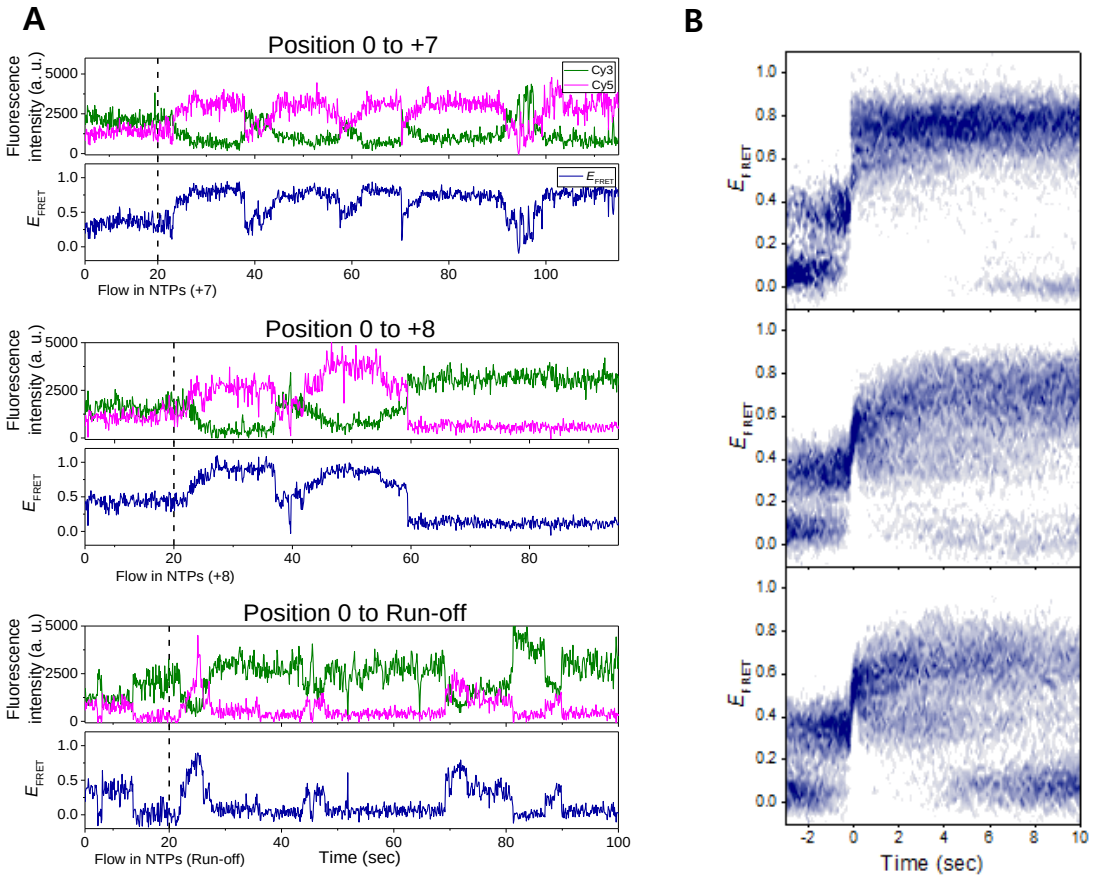

Figure 8. (A) Example traces from NTP flow-in experiments. The NTPs are added after 20 seconds from the beginning of the measurements (dashed line). First trace is coming from the position +7, second one is from position +8, and third one is coming from run-off condition. (B) FRET efficiency population graphs before and after the transition toward the efficiency higher than 0.5. The graphs are drawn with collected transitions from the flow-in experiments. From the top, position +7, position +8, and run-off conditions respectively.

3.3 Distinct level of FRET efficiency in position +8 complex

Because the level of FRET efficiency in position +8 is not well distinguished with the level of closed DNA. We designed an additional substrate DNA which is labeled with Cy3 and Cy5 at +11/-11 position respectively. By measuring the FRET efficiency upon the transcription as previously described, distinct level of the efficiency was observed at position +8 at 0.45. According to this, the 0.15 FRET efficiency at position +8 from +16/-16 labeled DNA was not coming from closed DNA, but protein-DNA complex that undergoes large structural change.

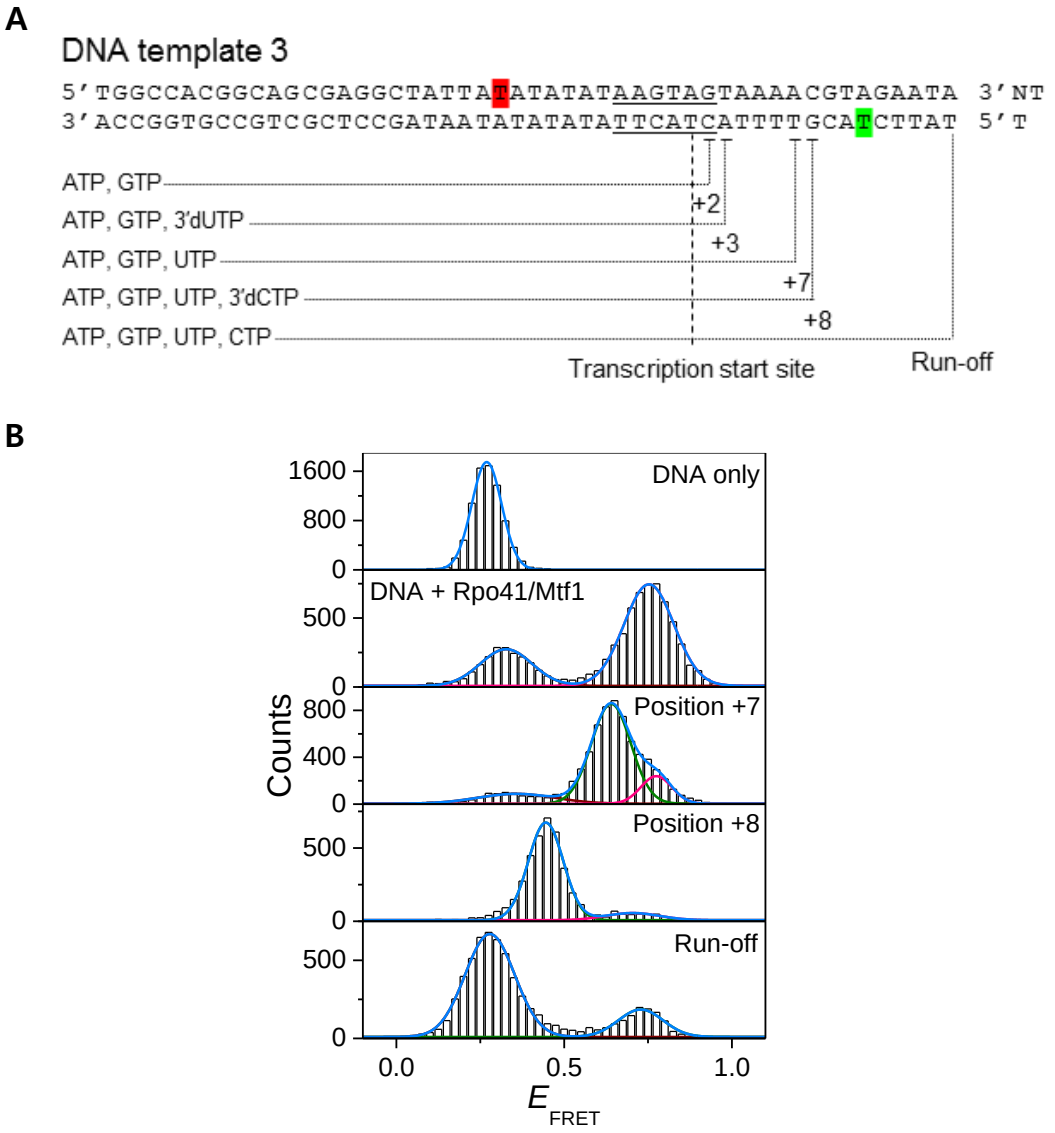

Figure 9. (A) Schematic view of the additional substrate DNA to distinguish the level of FRET efficiency in position +8. The donor of FRET, Cy3, is labeled on +11 position and the acceptor is labeled on -11 position from the transcription start site. (B) FRET efficiency histograms of the +11/-11 labeled DNA.

3.4 Hidden Markov Modelling analysis

In order to visualize the conformational dynamics along the initiation and elongation phases, we employed hidden Markov analysis of the smFRET traces (Fig. 9A). Traces from open promoter (position 0) and downstream positions revealed three-state dynamic transitions between closed/unbent DNA, open/bent DNA, and scrunched DNA conformations. The dynamics remained for certain time after washing off free NTP, showing that such dynamics persists in the presence of nascent RNA transcript within the complex. The coexistence of these conformations and the stepwise changes of the transition rates are well represented by the transition density plots (Fig. 9B), providing views on how the initiation complex progresses and makes transition to the elongation phase. Except the case that there are only 2 peaks, all positions are analyzed to have three different states, closed DNA with low FRET efficiency around 0.1(cyan), opened DNA with middle FRET efficiency around 0.4(orange), and scrunched DNA with high FRET efficiency larger than 0.5(purple) (Fig. 8A). The HMM analysis gave us meaningful information such as dwell time of each state, and transition rates among the three states. Based on the results, transition density plots (TDP) at each position are drawn. As you can see from the plots, without any NTPs, there is only dynamics between closed state low FRET and opened state middle FRET. However, if RNA transcribed 2 bp, the scrunching-unscrunching events between middle FRET and high FRET become dominant. The FRET level of scrunched state increases when the transcription proceeds. Another remarkable thing is that high FRET state and transition events disappear when the RNA transcribed 8 bp.

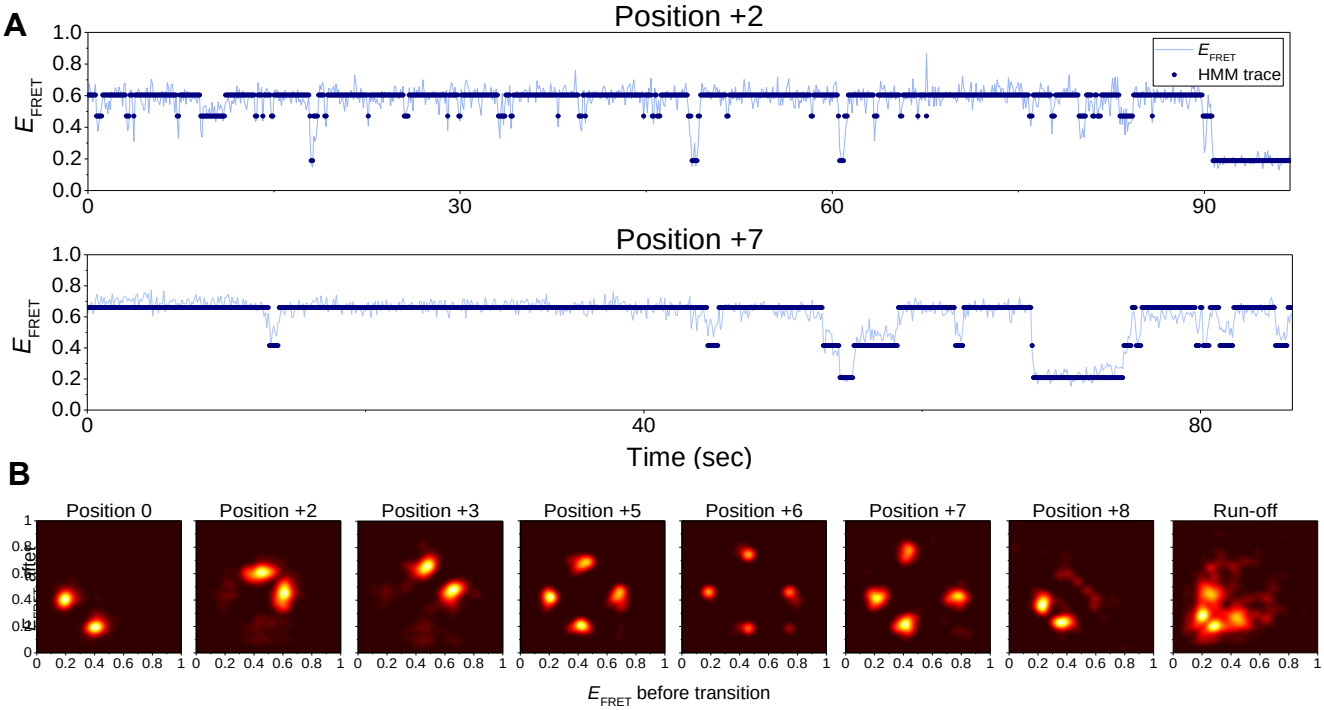

Figure 10. Hidden Markov Modelling (HMM) analysis. (A) Example panel showing HMM analysis. Three states are assigned properly. Closed DNA state (cyan), opened DNA state (orange), and scrunched DNA state (purple). (B) Transition density plots (TDP) at each position. It shows the density of transition from one state to another.

Transition rates at each position were analyzed by HMM. Bar graph is showing that at the very first stage of transcription, the FRET level is more likely to become higher state (2→3, yellow bar). However, the transition rate from 2 state to 3 state is decrease when RNA transcribed 3 bp. Interestingly, at the position +8, the transition rate from state 3 to 2 is dramatically increase, which means that the complex does not maintain high FRET conformation. This can be another evidence that the phase transition from initiation to elongation happens at this point.

Transition Rates	k_{12}	k_{13}	k_{21}	k_{23}	k_{31}	k_{32}
0	0.02483	N/A	0.01251	N/A	N/A	N/A
2	0.02814	0.003158	0.06282	0.1603	0.00221	0.02882
3	0.08034	0.00128	0.02224	0.03558	0.003169	0.02284
5	0.02049	0.003363	0.02552	0.04551	0.001587	0.01299
6	0.02441	0.005178	0.0323	0.04029	0.002112	0.01332
7	0.009873	0.001058	0.02099	0.02384	0.000848	0.007096
8	0.01367	0.000633	0.01662	0.02081	0.009473	0.1547
16	0.01056	0.003354	0.01726	0.02147	0.01962	0.07413

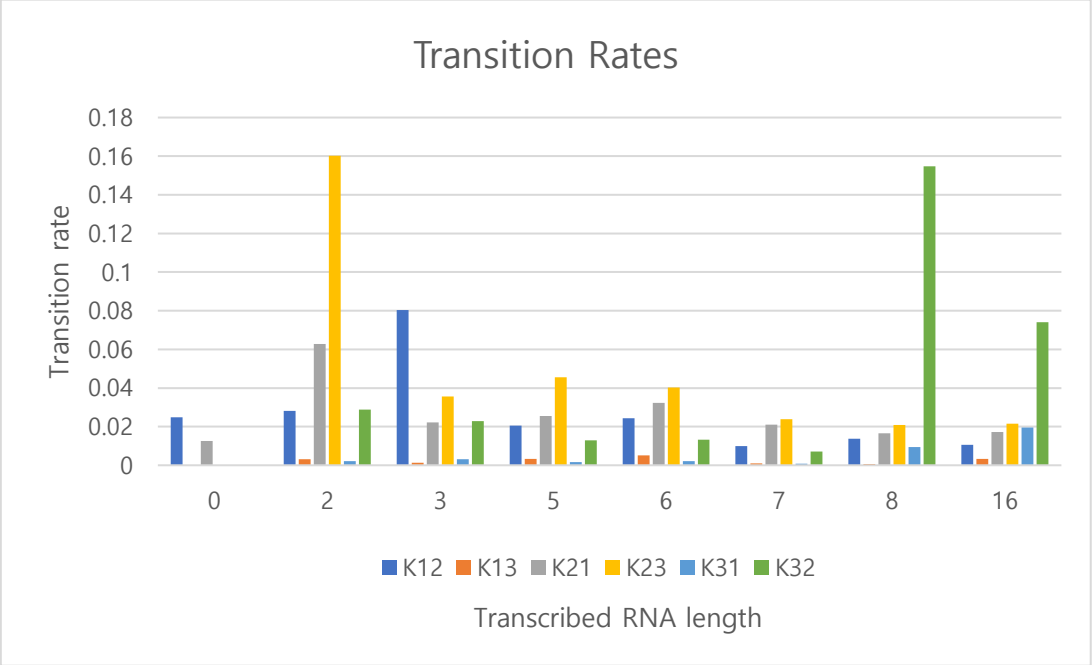

Figure 11. (Table) The table shows the transition rates at each position from HMM analysis and plotted into bar graph. There are three states (state 1 closed DNA, state 2 opened DNA, and state 3 scrunched DNA) during transcription at each stalled position. (Bar graph) Comparison of transition rates among the three states at each position.

3.5 Role of C-terminal tail of Mtf1 at initiation phase

Additional control experiment using mutant Mtf1 was done to figure out the role of C-terminal tail of Mtf1 in the initial stage of the transcription. The C-terminal tail region of Mtf1 was truncated 12 amino acids (D12-Mtf1) and 20 amino acids (D20-Mtf1). Because of low activity of D20-Mtf1, smFRET measurements were done only with D12-Mtf1. The histograms and example traces here, are showing that the IC without C-terminal tail of Mtf1 the complex cannot maintain high FRET level (Fig. 11A & B). By using radiolabeled phosphate ATP (γ^{32}-ATP), transcription gel assays were done. (Fig. 11C) The DNA template used here is same with the DNA which was used in single molecule measurements. Similarly, the transcription can be stalled at each point by adding different combinations of NTPs to the reaction. We have confirmed that the transcription with our substrate DNA occurs well and can be stalled at the desired positions. (In the right-hand gel when the NTP combination with +7 position added, there is 'slippage' effect that synthesize RNA over 7-mer. This is because of multiple sequential 'A' on the substrate DNA sequence.) By doing this gel assay, we could know that the overall activity of transcription by C-tail deleted mutant Mtf1 is lower than wild-type and make less abortive products.

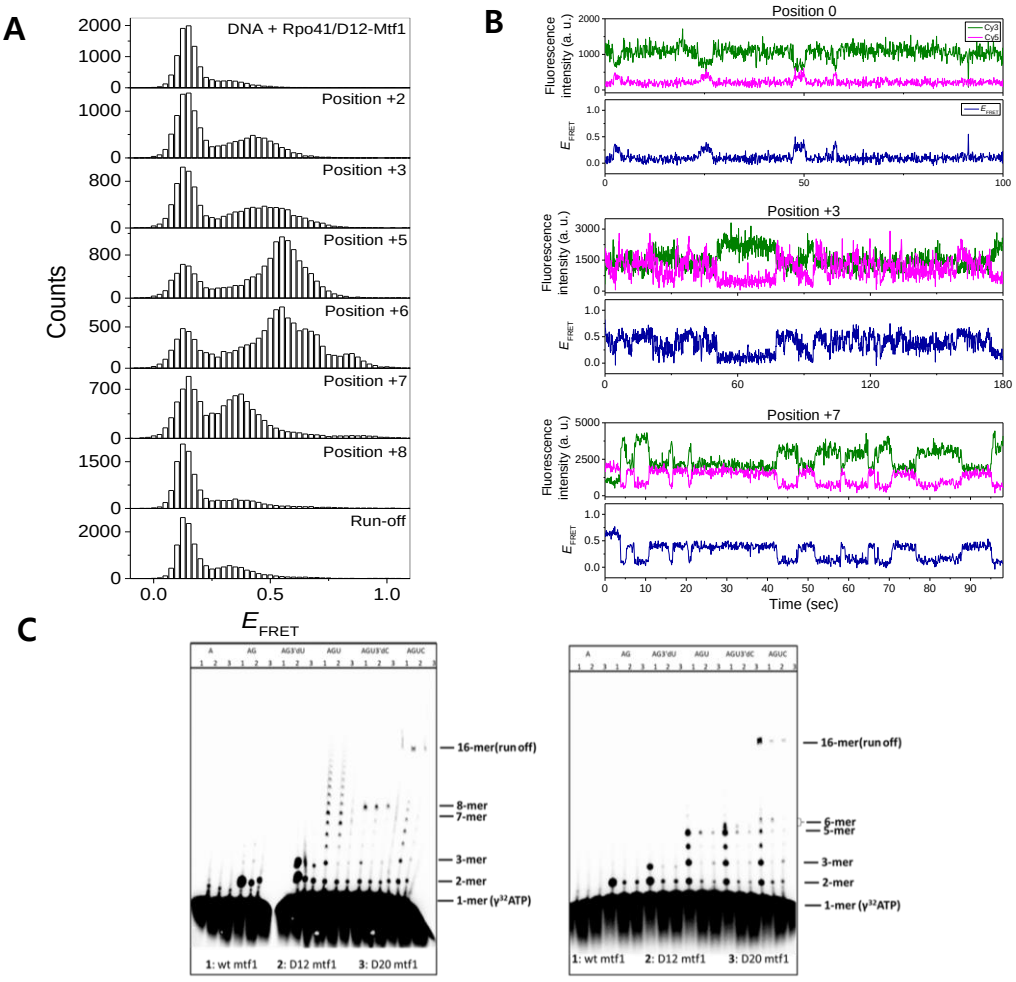

Figure 12. (A) FRET histograms from experiments using mutant D12-Mtf1 at each stalled position. (B) Example FRET trace from D12-Mtf1 measurements. (C) Transcription gel assay using γ^{32}-ATP as substrate of transcription. Three lines from left to right are 1 WT-, 2 D12-, and 3 D20-Mtf1 and this order repeats.

3.6 NTP washing experiments

To observe abortive transcription during the initiation process, we did an additional experiments. After make the transcription reaction to reach equilibrium, the NTPs were washed out from the reaction chamber and the FRET efficiency was measured from right after the washing to 5 miniutes. From the histograms, at position +2 the peak about 0.6 in equilibrium state already disappear rigth after the washing (first column, Fig. 13A). However, in the case of position +7, the high FRET peak remains even after 5 minutes from the washing (second column, Fig. 13A). In position +8, it seems that the shape of histograms didn't change at all (third column, Fig. 13A). To validate the 0.15 peak at position +8 is unique peak of position +8, we did same washing expereiment with +11/-11 labeled DNA, and confirmed the peak of position +8 is maintained for longer time (fourth column, Fig. 13A). Because the binding of nascent RNA and template strand of the DNA become stronger if the length of the RNA is longer, the time of maintaining the structure is longer in position +7 or +8. (Fig. 13B)

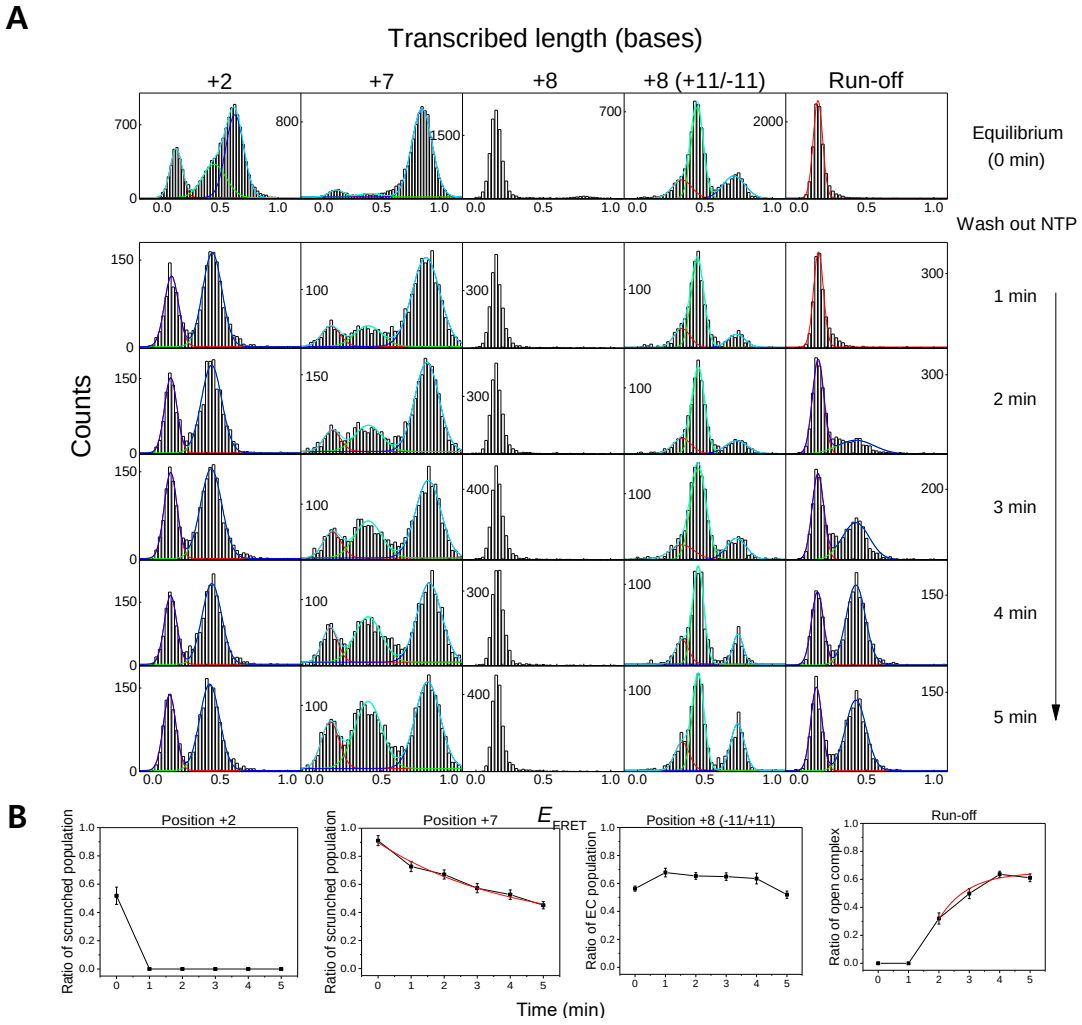

Figure 13. (A) FRET efficiency histograms from washing experiments. The histograms on the top row come from equilibrium states of 4 different stalled positions and run-off condition. The bottom part is showing population change in the histograms until 5 minutes after washing out the NTPs. (B) Graphs comparing change in the population of FRET efficiency population after the washing at each position.

4. Discussion & Conclusion

We employed single molecule techniques combined with biochemical studies to probe the dynamics during the initiation and elongation phases of transcription machinery. We have observed the conformational dynamics at each transcriptional step and revealed how the mitochondrial transcription machinery controls the transition to the elongation phase by modulating the dynamics of the initiation complex. Our results provide novel mechanistic perspective on how transcription process is regulated in multi-protein eukaryotic transcription machineries beyond single-protein transcription systems.

To further our research, we are planning to observe human mitochondrial system which has three proteins in its transcription. Unlike POLRMT or TFB2M, there was no homologous protein to TFAM in the yeast system. By observing conformational changes or dynamics among states in human system, the role of TFAM in transcription can be elucidated.

5. References

1. Matsunaga, M., Jang, S. H., & Jaehning, J. A. (2004). Expression and purification of wild type and mutant forms of the yeast mitochondrial core RNA polymerase, Rpo41. *Protein expression and purification*, *35*(1), 126-130.
2. Tang G.Q., Paratkar S., Patel S.S.. Fluorescence mapping of the open complex of yeast mitochondrial RNA polymerase, J. Biol. Chem. 2009, vol. 284 (pg. 5514-5522)
3. Chandradoss, S. D., Haagsma, A. C., Lee, Y. K., Hwang, J. H., Nam, J. M., & Joo, C. (2014). Surface passivation for single-molecule protein studies. Journal of visualized experiments: JoVE, (86).
4. Wade, J. T., & Struhl, K. (2008). The transition from transcriptional initiation to elongation. *Current opinion in genetics & development*, *18*(2), 130-136.
5. Jang, S. H., & Jaehning, J. A. (1991). The yeast mitochondrial RNA polymerase specificity factor, MTF1, is similar to bacterial sigma factors. *Journal of Biological Chemistry*, *266*(33), 22671-22677.
6. Nayak, D., Guo, Q., & Sousa, R. (2009). A promoter recognition mechanism common to yeast mitochondrial and phage t7 RNA polymerases. *Journal of Biological Chemistry*.
7. Schubot, F. D., Chen, C. J., Rose, J. P., Dailey, T. A., Dailey, H. A., & Wang, B. C. (2001). Crystal structure of the transcription factor sc-mtTFB offers insights into mitochondrial transcription. *Protein Science*, *10*(10), 1980-1988.
8. Falkenberg, M., Gaspari, M., Rantanen, A., Trifunovic, A., Larsson, N. G., & Gustafsson, C. M. (2002). Mitochondrial transcription factors B1 and B2 activate transcription of human mtDNA. *Nature genetics*, *31*(3), 289.
9. Eddy, S. R. (2004). What is a hidden Markov model?. *Nature biotechnology*, *22*(10), 1315.
10. McKinney, S. A., Joo, C., & Ha, T. (2006). Analysis of single-molecule FRET trajectories using hidden Markov modeling. *Biophysical journal*, *91*(5), 1941-1951.
11. Koh, H. R., Roy, R., Sorokina, M., Tang, G. Q., Nandakumar, D., Patel, S. S., & Ha, T. (2018). Correlating Transcription Initiation and Conformational Changes by a Single-Subunit RNA Polymerase with Near Base-Pair Resolution. *Molecular cell*, *70*(4), 695-706.
12. Kim, H., Tang, G. Q., Patel, S. S., & Ha, T. (2011). Opening–closing dynamics of the mitochondrial transcription pre-initiation complex. *Nucleic acids research*, *40*(1), 371-380.
13. Tang, G. Q., Roy, R., Bandwar, R. P., Ha, T., & Patel, S. S. (2009). Real-time observation of the

transition from transcription initiation to elongation of the RNA polymerase. *Proceedings of the National Academy of Sciences*, pnas-0906979106.